Figure S1. Cross-referencing the ROH regions identified by the fine-tuned BAFCalculator to the array data ROH calls in the HGDP dataset gave us a positive predictive value of 90% and true positive rate of 72% when the seg.mean parameter=0.47.

Figure S2. Comparison of FROH (the total size of ROHs >= 1.5 Mb) estimates identified from those regions (FROH_ES) to the FROH estimates identified from the genome sequencing data (FROH_GS). These analyses showed us that when the seg.mean=0.47, this gives us nearly perfect correlation (0.98) between FROH_ES and FROH_GS and ES performs similarly to GS.

Figure S3. Comparison of ancestry component fractions between the TK cluster 1 (N=285) and cluster 2 (N=1,131) individuals. We compared the admixture proportions of the TK cluster 1 and cluster 2 individuals in terms of A) African, B) East Asian, C) European, D) South Asian and E) Other ancestry component fractions.

Figure S4. TK variome compared to gnomAD African, East Asian, European and South Asian subpopulation variomes. The pie charts show the comparison of all distinct variants represented in the TK **B)** unaffected cluster 1; **C)** unaffected cluster 2; **D)** affected cluster 1 and **E)** affected cluster 2 to the genome aggregation database (gnomAD) African (AFR) (first panel), East Asian (EAS) (second panel), European (EUR) (third panel) and South Asian (SAS) (bottom panel) subpopulation variome.

Figure S5. Genomic distribution of ROH regions in the TK cohort.

The density of ROH regions present in the TK affecteds and unaffecteds were depicted as a circus plot on each chromosome.

Figure S6. Genomic size features of ROHs detected in the TK cohort.

The features of A) medium-sized, B) short-sized and C) total ROHs were displayed irrespective of their total size (Mb) (left panel), the number of ROH blocks (middle panel) and the median length of ROH blocks (Mb) (right panel). In each panel, horizontal boxplots compare the two individual groups as the TK affected (TK-aff) and unaffected (TK-unaff) individuals. A one-sided Wilcoxon rank sum test was used to test the difference in the TK-affected versus TK-unaffected individuals and is indicated to the right of each panel.

Figure S7. Correlation between total ROH span and the estimated F values in the TK cohort. The scatterplots show the relationship between the estimated F values (y-axis) and the total length of **A)** long-sized, **B)** medium-sized and **C)** short-sized ROHs (x-axis) for the TK affected (TK-aff) and TK unaffected (TK-unaff) individuals.

Figure S8. **Total ROH burden among the TK affected and unaffected cluster 1 and 2 individuals.** Boxplots show the total length of ROH segments (Mb) in each size category (**A)** long-sized, **B)** medium-sized, **C)** short-sized and **D)** total ROH in 4 subject groups including the TK affected cluster 1 (TKaff-cluster1) and cluster 2 (TKaff-cluster2) individuals and the TK unaffected cluster 1 (TKunaff-cluster1) and cluster 2 (TKunaff-cluster2) individuals.

Figure S9. **Deleterious variant density among the TK affected and unaffected cluster 1 and 2 individuals.** Boxplots display rare homozygous deleterious variant density manifested in each ROH size category (**A)** long-sized, **B)** medium-sized, **C)** short-sized ROHs and **D)** non-ROHs in 4 subject groups including the TK affected cluster 1 (TKaff-cluster1) and cluster 2 (TKaff-cluster2) individuals and the TK unaffected cluster 1 (TKunaff-cluster1) and cluster 2 (TKunaff-cluster2) individuals.

Figure S10. Correlation between deleterious variant densities in ROHs and estimated F values. The scatterplots show the relationship between the estimated F values (x-axis) and the rare homozygous deleterious variant density presented in **A)** long-sized, **B)** medium-sized and **C)** short-sized ROHs (y-axis) for the TK affected (TK-aff) and TK unaffected (TK-unaff) individuals.

Figure S11. Long-sized ROH regions with increased density of rare deleterious variants are enriched in TK affecteds. We calculated a variant density metric by normalizing the count of rare homozygous deleterious variants to the count of rare homozygous synonymous variants. The density of rare homozygous deleterious variants manifested in long-sized, medium-sized, short-sized ROH regions and not ROH (non-ROH) regions in the TK affecteds (TK-aff) and TK unaffecteds (TK-unaff) subgroups. We then compared the rare homozygous deleterious variant density between the TK-aff and TK-unaff subgroups in each ROH size group and non-ROHs. P-value significance levels were marked on the top of each pair of groups compared (*<0.05, **<0.01, ***<0.001, ****<0.0001). Outliers were not shown in the boxplots.

Supplementary Figure 1

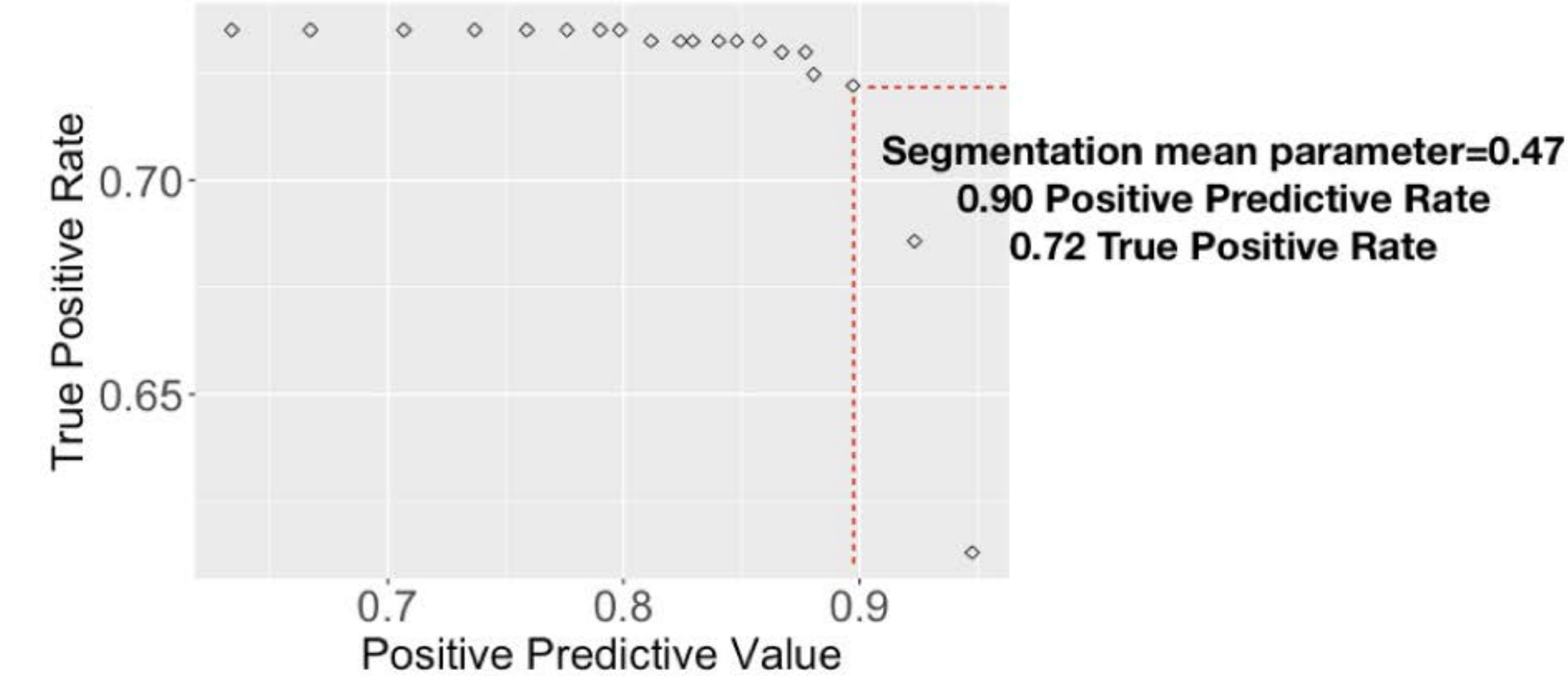

Supplementary Figure 2

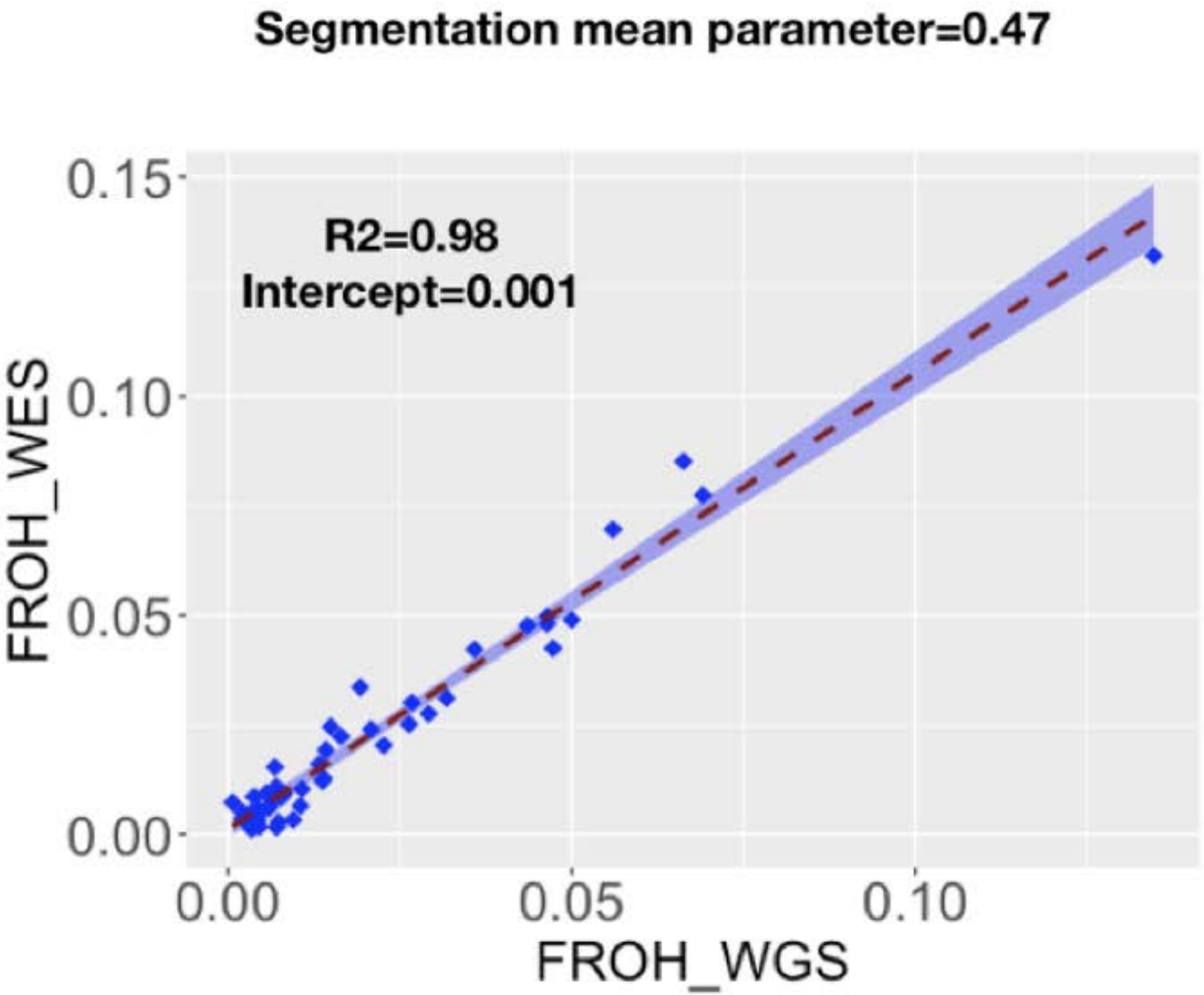

Supplementary Figure 3

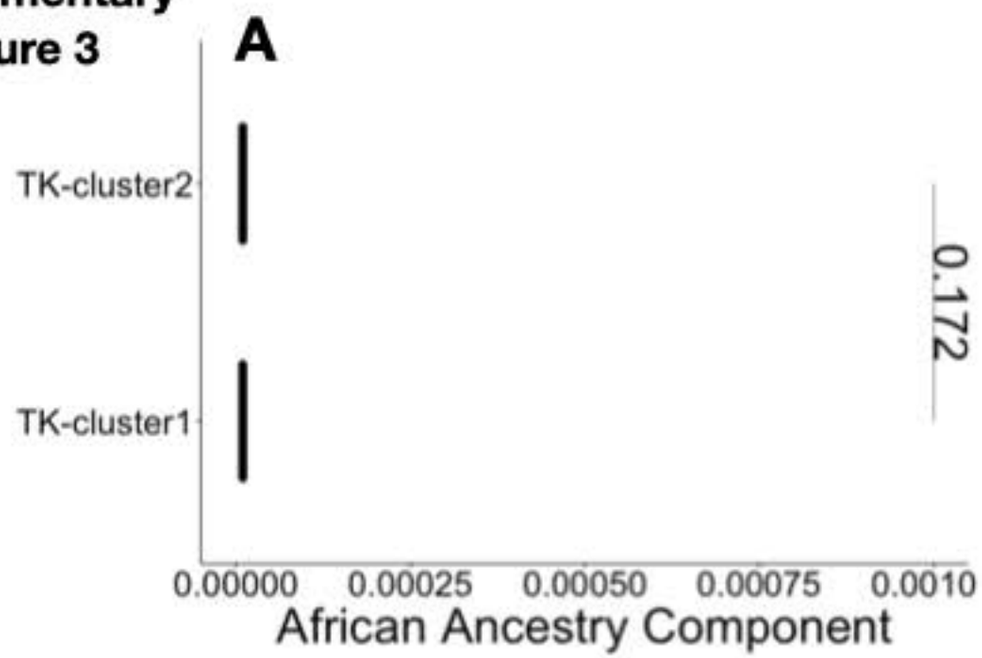

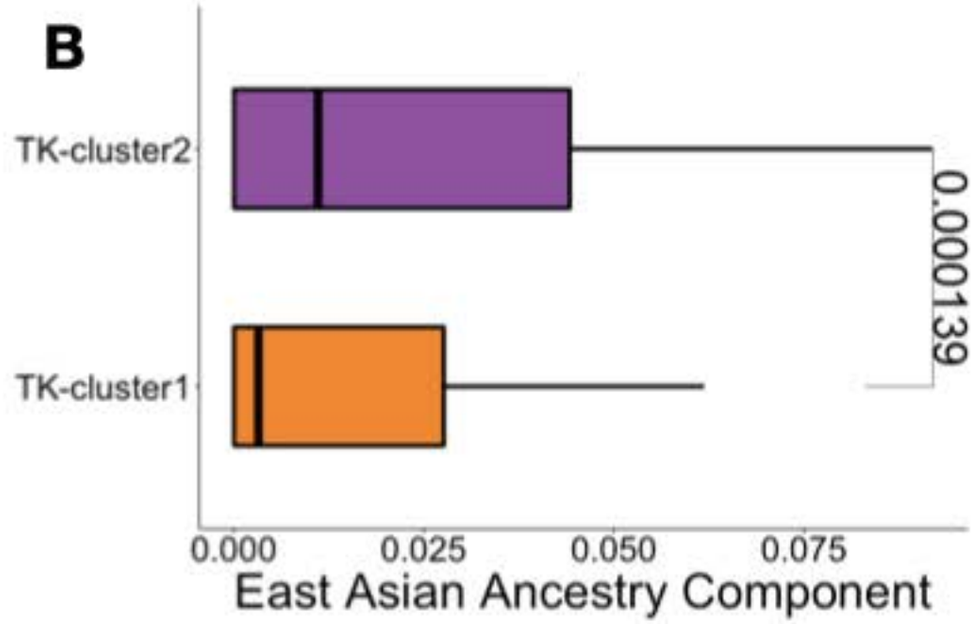

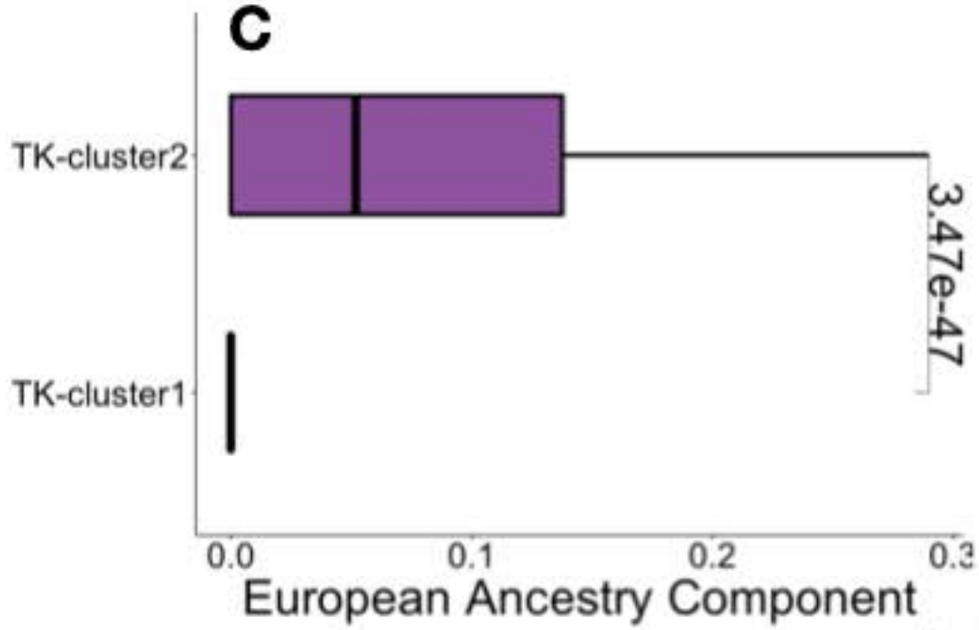

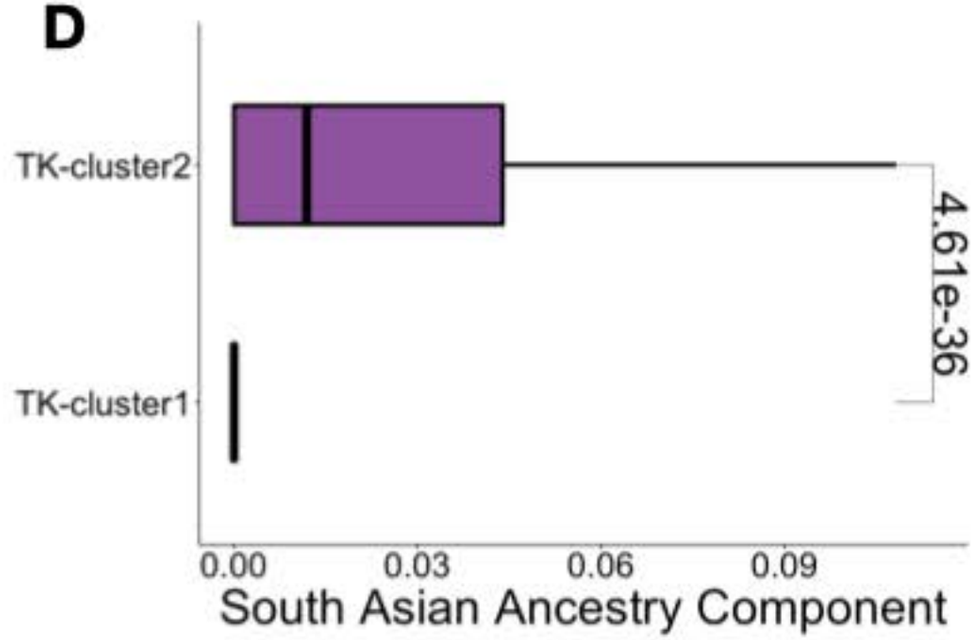

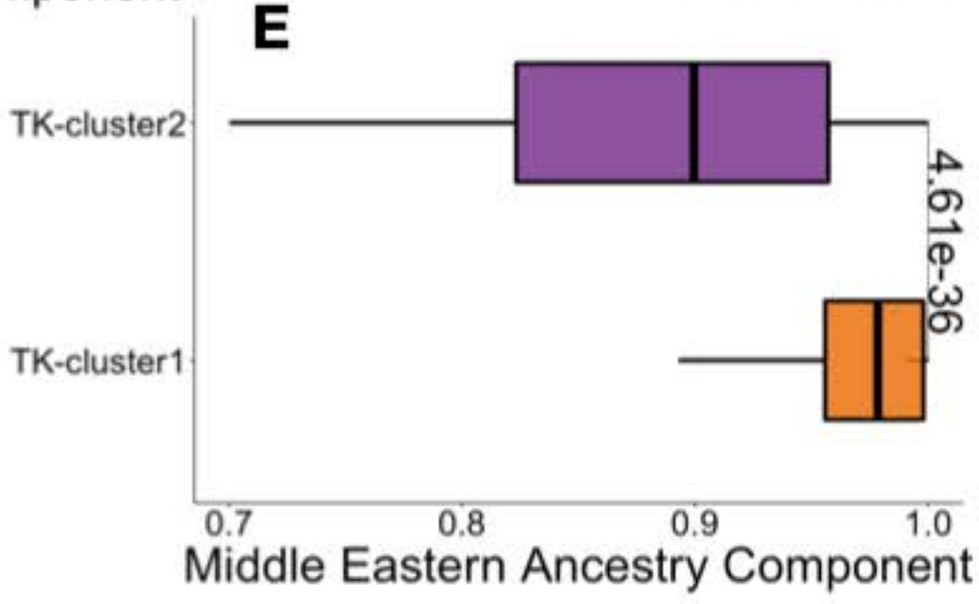

Supplementary Figure 5

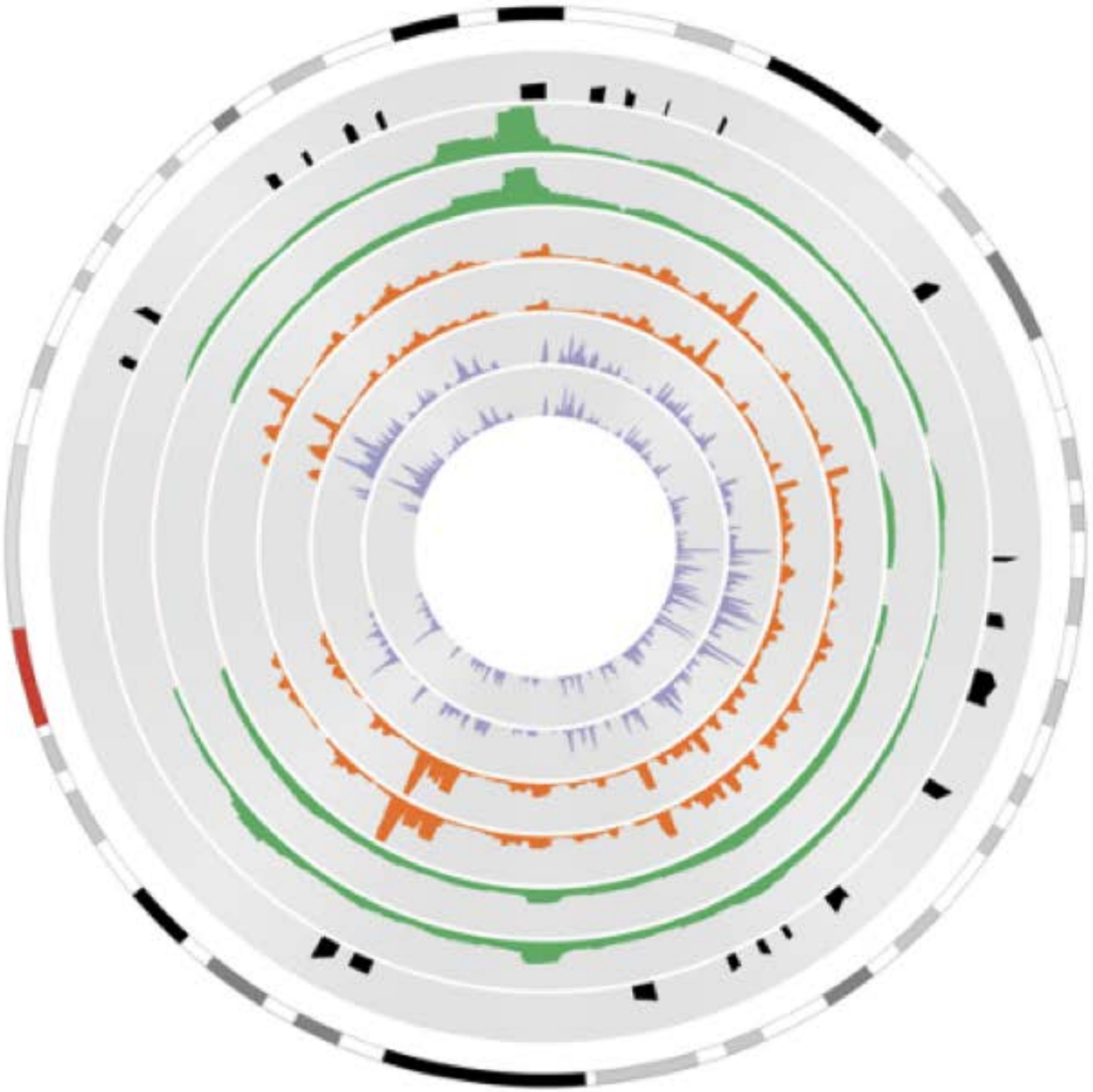

Supplemental Figure 6

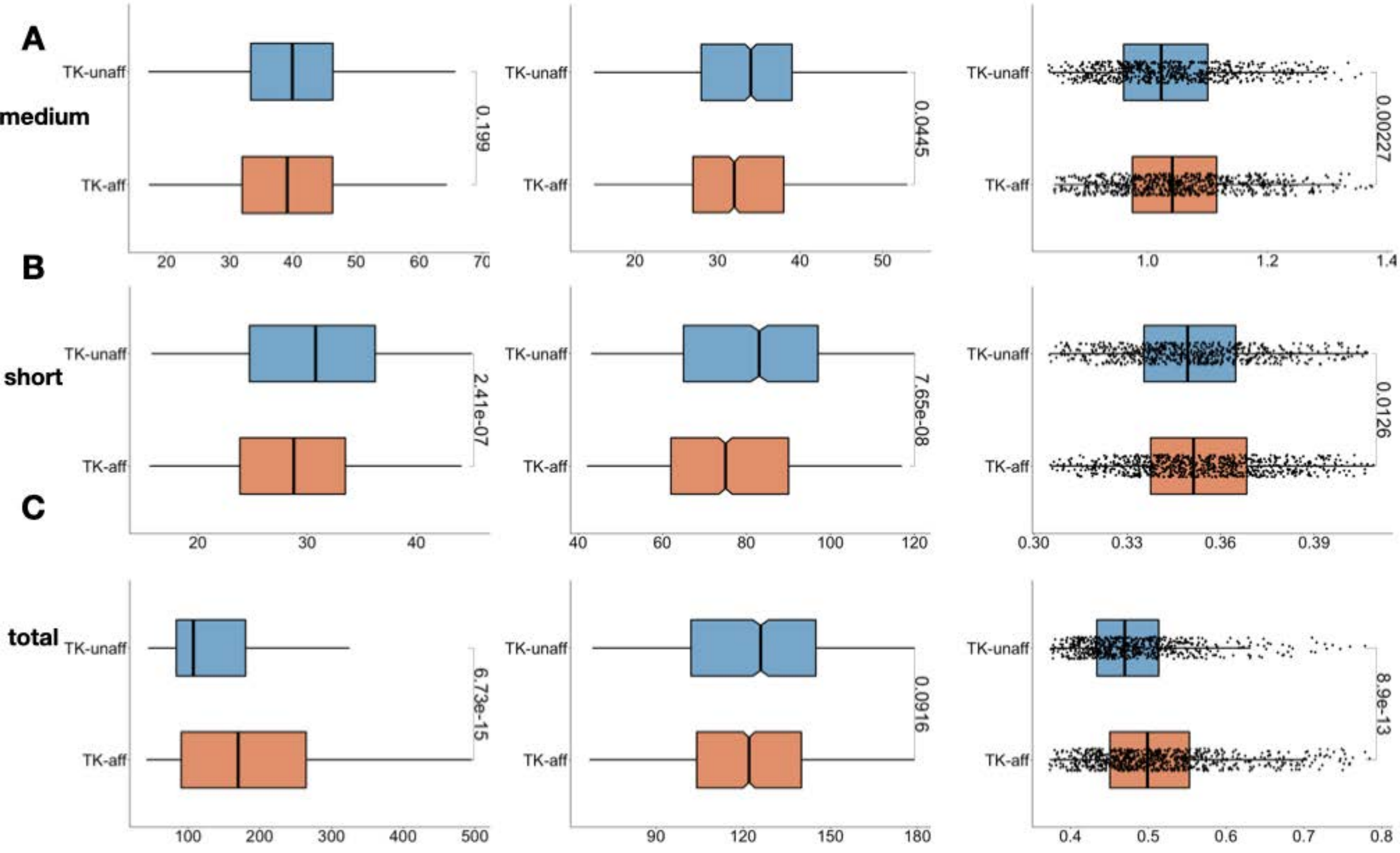

Supplementary Figure 7

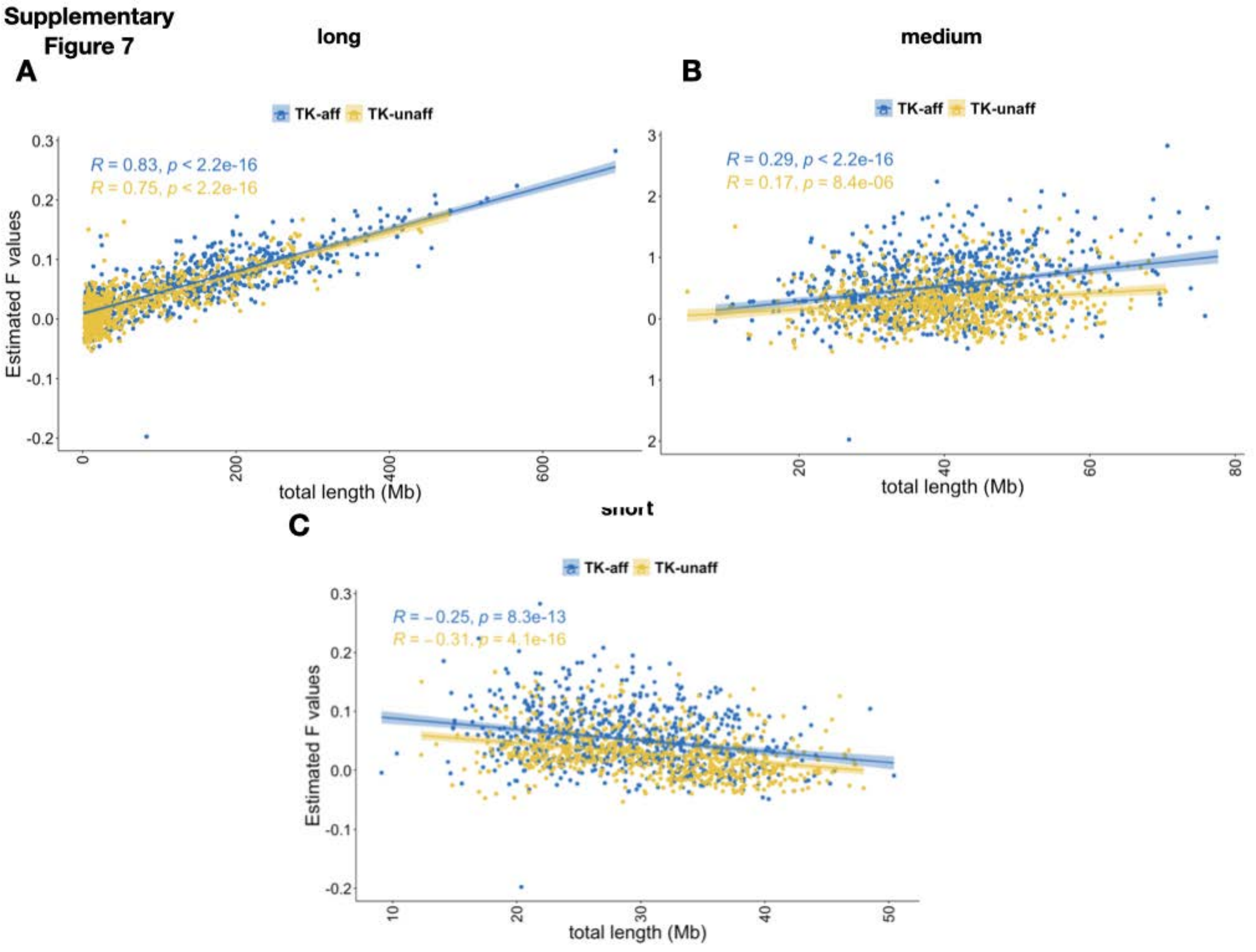

Supplementary Figure 8

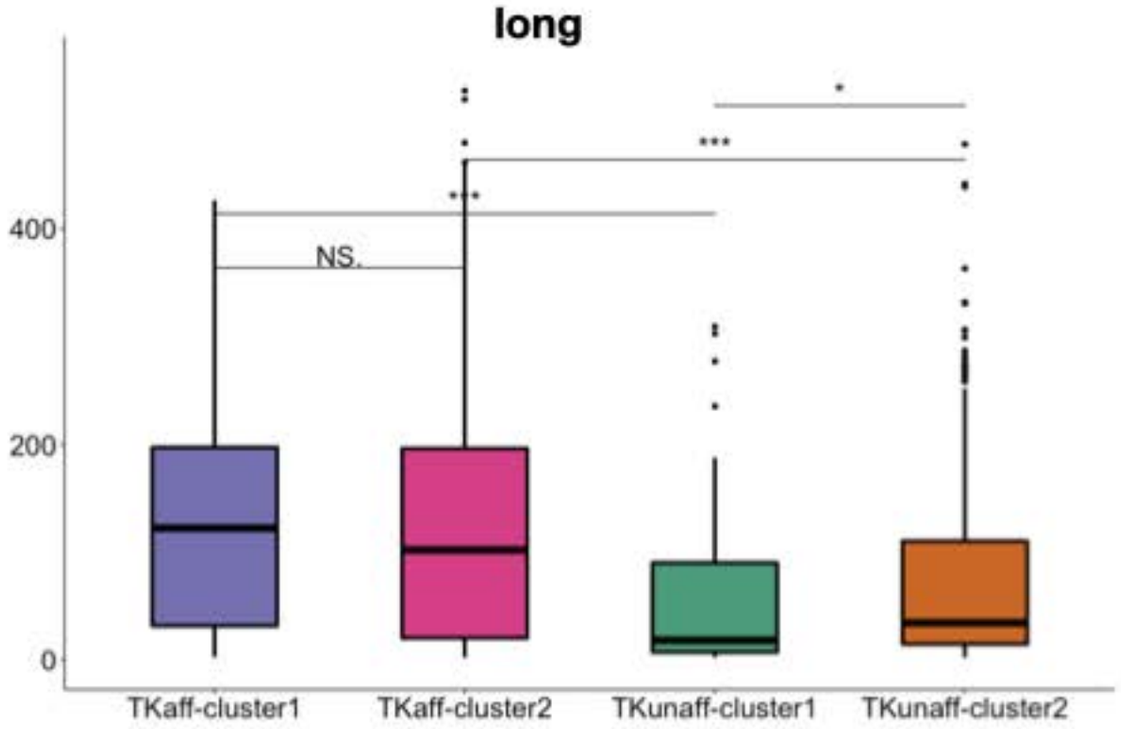

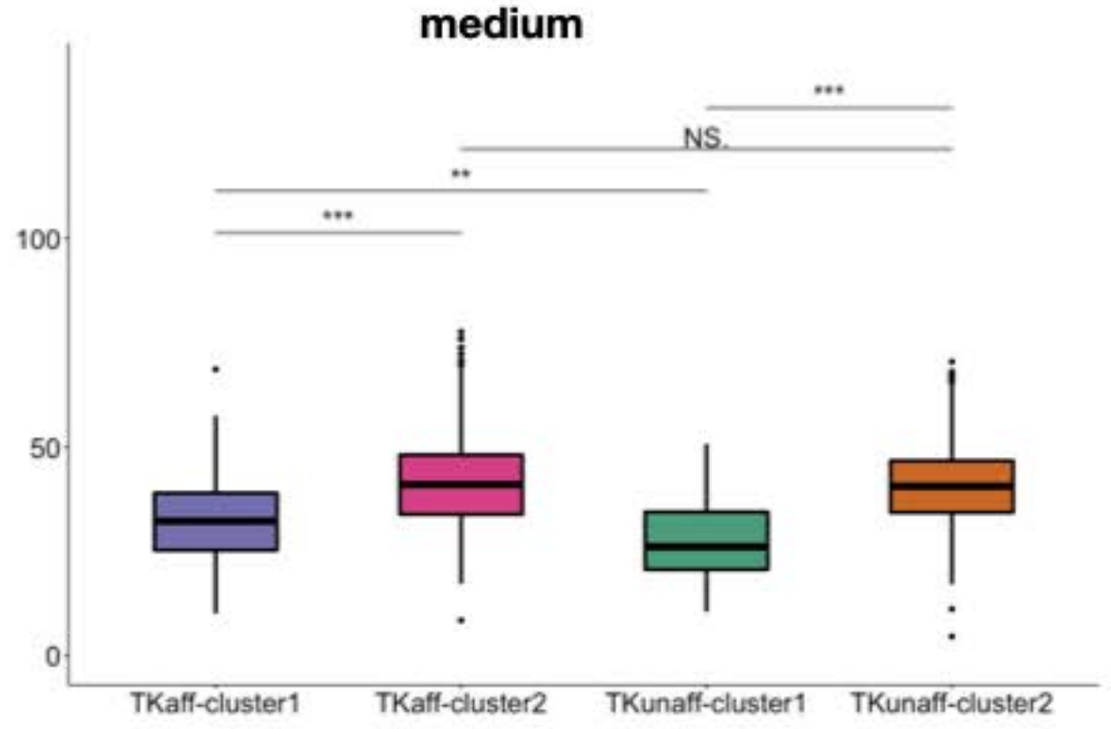

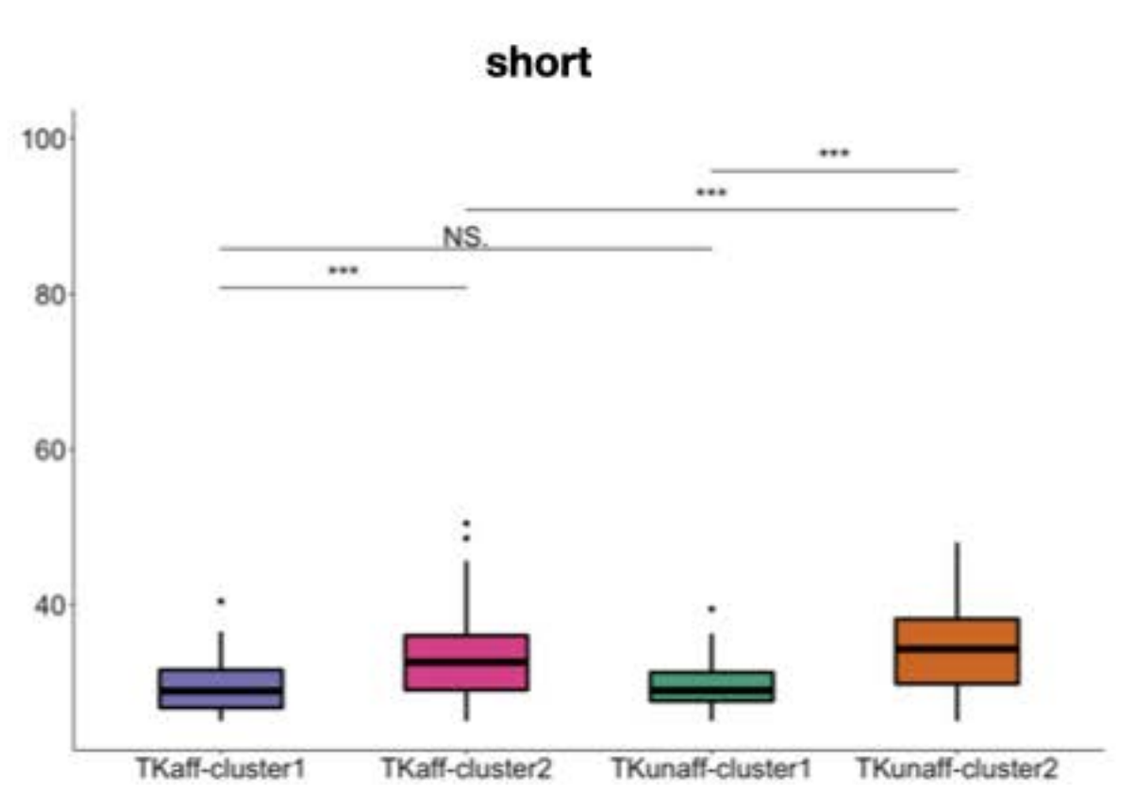

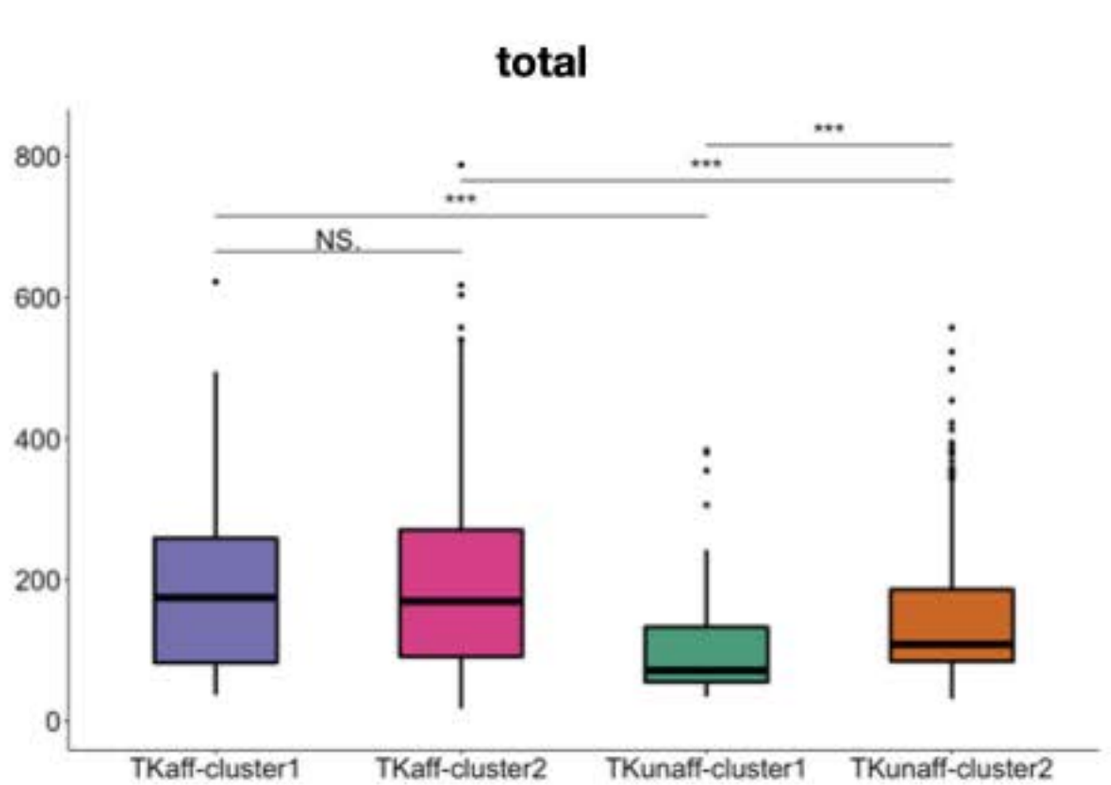

Supplementary Figure 9

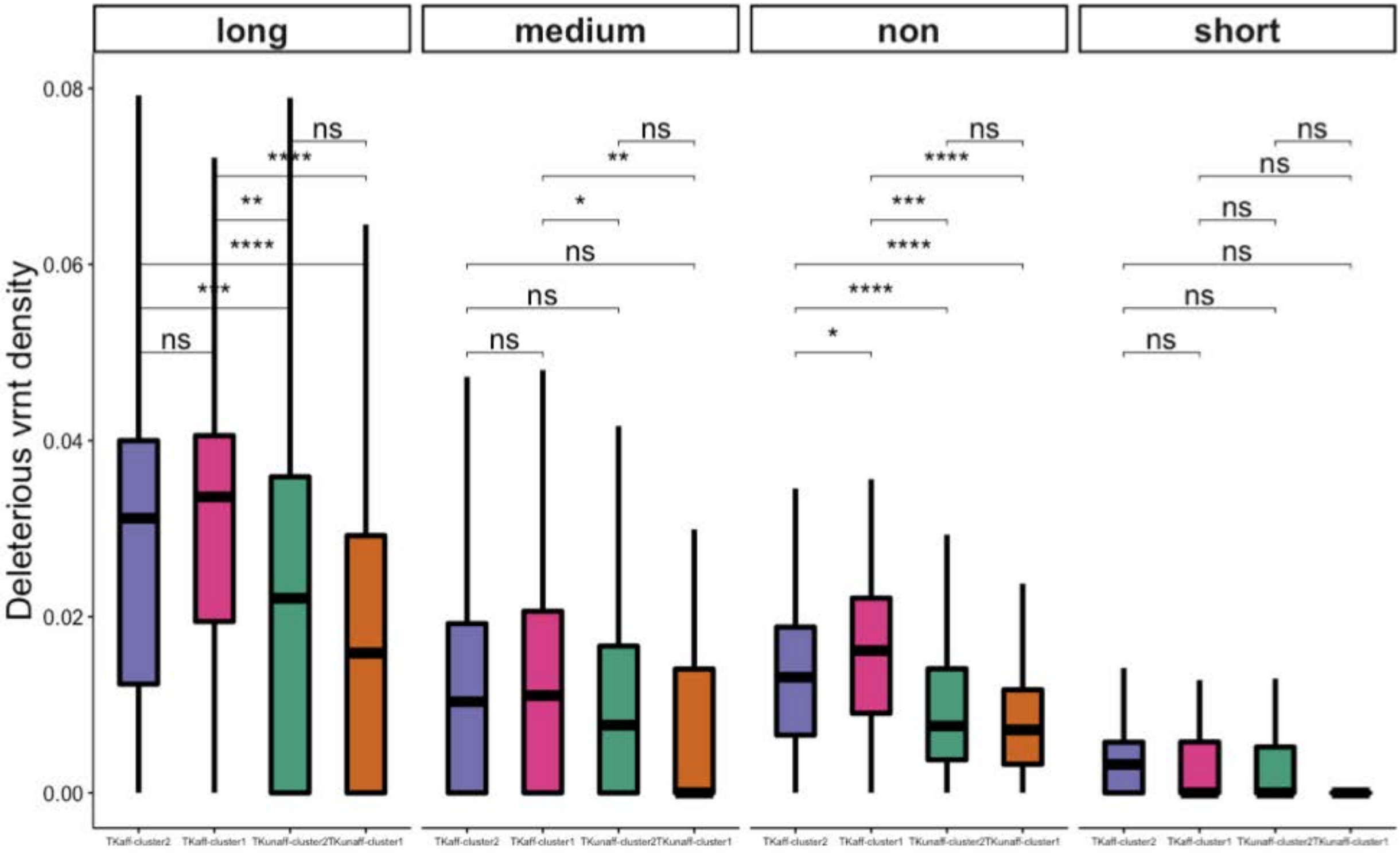

Supplementary Figure 10

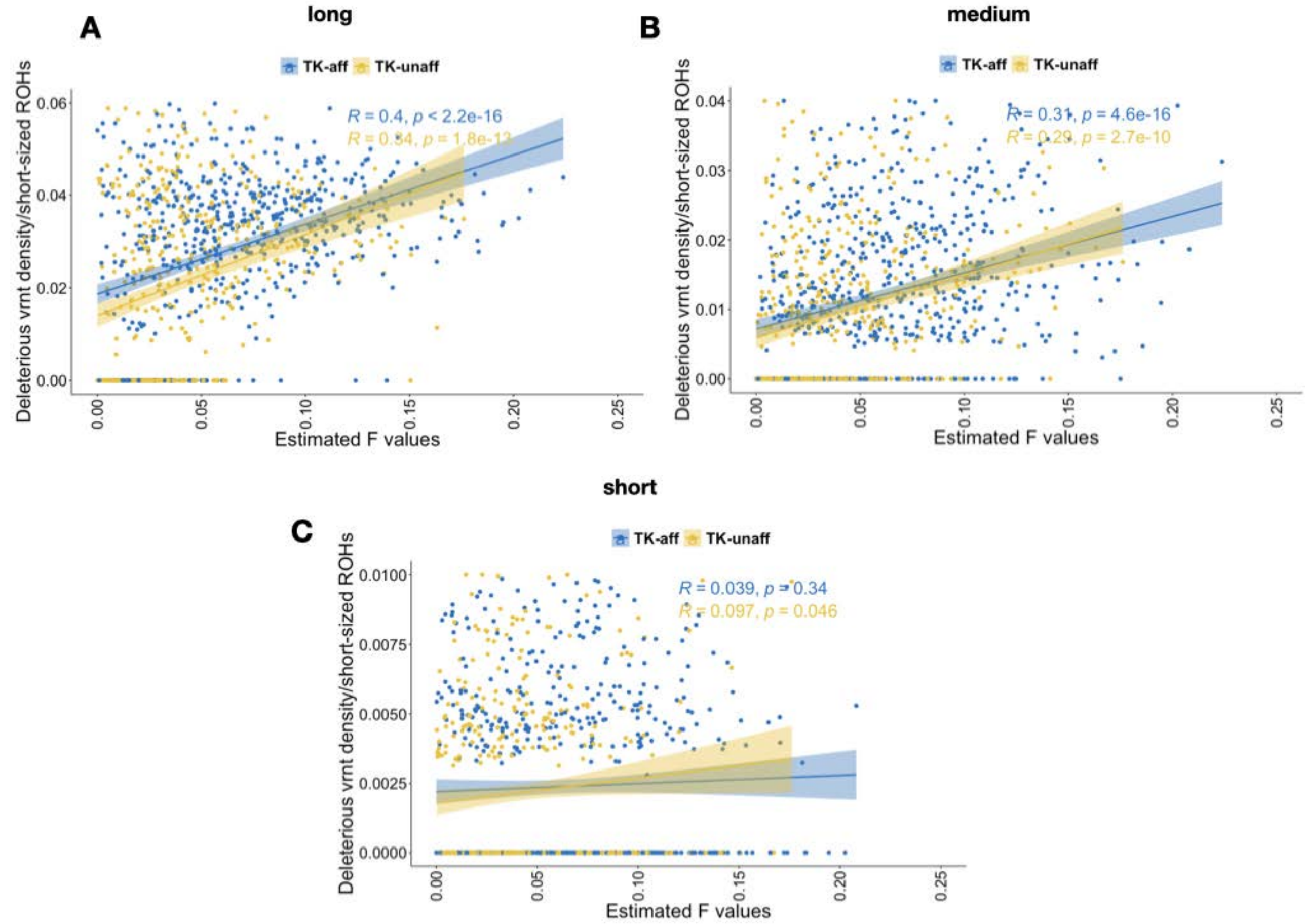

Supplementary Figure 11